Journal of Animal and Veterinary Advances 13 (8): 538-544, 2014
ISSN: 1680-5593

Enhancing Catalytic Activity of a Xylanase Retrieved from a Fosmid Library of Rumen Microbiota in Hu Sheep by Directed Evolution

Wen Du, Qian Wang, Jia-Kun Wang and Jian-Xin Liu
Institute of Dairy Science, College of Animal Science, Zhejiang University, 310058 Hangzhou, China

Abstract: The catalytic activity of a xylanase retrieved from a Fosmid Library of rumen microbiota in Hu sheep was improved by directed evolution using error-prone PCR. After the first round of random mutagenesis, one (C12) was selected from 1450 clones. And E12 with the highest activity was acquired from about 2500 clones in the second round. The specific activity of purified mutant C12 and E12 was 69.67 and 118.50 U mg^{-1}, 1.2 and 2.0 times as that of its parent enzyme HA2, respectively. The optimum temperature of Wild Type (WT) and mutants were 50°C while the mutants displayed lower thermostability than WT. The optimum pH for HA2, C12 and mutant E12 was 5.0, 5.0 and 6.0, respectively. Both WT and mutants retained about 85% of initial activity at pH range from 5.0-9.0. Sequencing analysis revealed that C12 was mutated at two amino acid positions (Q14H and K57R) and E12 was mutated at Q14H, V20A, M53I and K57R. Compared to HA2, the mutation of Q14H and K57R increased the affinity of xylanase to substrate (km was changed from 11.22-2.42 mg mL^{-1}) decreased catalytic efficiency (kcat from 42.82-9.82 sec^{-1}). Nevertheless, further mutation of V20A and M53I reversed the km to 45.14 mg mL^{-1} and kcat to 198.75 sec^{-1} which suggested that V20A and M53I probably contributed to the enhanced activity.

Key words: Xylanase, rumen, catalytic activity, directed evolution, error-prone PCR

INTRODUCTION

Xylanases (EC 3.2.1.8) are a set of glycosidases that catalyze the hydrolysis of xylan, a major constituent of hemicellulosic polysaccharide. Xylanases have been widely used in the food, feed, fuel, textile and paper and pulp industries (Beg *et al*., 2001).

Usually, the activity of xylanases isolated from nature is too low to satisfy the demands for industrial applications and properties of xylanases should be further improved through protein engineering using techniques such as site-directed mutagenesis and directed evolution (Stephens *et al*., 2007; Wang *et al*., 2012a). Directed evolution which does not require high resolution of the three-dimensional structures of the enzyme is a powerful strategy of protein engineering and enzyme modification (Brakmann, 2001).

Rumen is a good resource to discover new *xylanase* gene for the large amount of microorganisms existed in it. To discovery new *xylanase* genes in rumen, a Fosmid Metagenomic Library was previously constructed from rumen samples of Hu sheep and one family 11 *xylanase* gene (*ORF6*) with high activity was identified using shotgun sequencing (Wang *et al*., 2012b). The xylanase encoded by this gene contains a catalytic domain of 233 amino acid residues and an unknown domain joined by a linker. To improve the catalytic activity of this new xylanase, two rounds of random mutagenesis were performed to construct mutant gene libraries using error-prone PCR and a high-throughout screening system based on 96 well plate was demonstrated to select variants with enhanced activity.

MATERIALS AND METHODS

Cloning of *xylanase* gene: The catalytic domain of the *xylanase* gene *ORF6* was amplified by PCR using the primers ORF6-UN-C (5'-GACGAAGCTTCCGCCCCCTC GATATAGACCT-3') and ORF6-UN-N (5'-TGACGGATC CGATTTTTGTCAAACTGCCGC-3') (Wang *et al*., 2012b). The PCR cycling conditions consisted of an initial step of 5 min at 94°C followed by 30 cycles of 0.5 min at 94°C, 0.5 min at 58°C and 80 sec at 72°C and a final extension step of 7 min at 72°C. After PCR reaction, the amplified products were purified using Cycle Pure kit (Omega, USA) and digested with Hind III and Bam HI (TaKaRa, Dalian, China) and then ligated with T4 DNA ligase into Hind III-Bam HI restriction site of pET-30a (Novagen, Germany) to generate the plasmid pET-30a-ORF6-UN. Finally they were transformed into *E. coli* BL21 (DE3) (Tiangen, Beijing, China) by heat shock.

Corresponding Author: Jia-Kun Wang, Institute of Dairy Science, Zhejiang University, Yuhangtang Road# 866, Hangzhou, Zhejiang, China

Construction of mutant library: Error-prone PCR was used to construct the randomly mutated ORF6-UN library (Miyazaki *et al*., 2006). The PCR was carried out according to the user manual of the Diversify™ PCR random mutagenesis kit (Clontech, Mountain View, CA, USA). Buffer condition 5 which is supposed to generate 4.6 mutation sites per 1000 bp was employed. The PCR mixture (50 μL) was composed of 40 mmol L^{-1} Tricine-KOH (pH 8.0), 16 mmol L^{-1} KCl, 3.5 mmol L^{-1} $MgCl_2$, 3.75 μg mL^{-1} Bovine Serum Albumin (BSA), 0.64 mmol L^{-1} $MnSO_4$, 40 μmol L^{-1}dGTP, 1×Diversify™ dNTP mix, 10 μmol L^{-1} concentrations each of flanking primers, 1 ng of pET-30a-ORF6-UN and 5 units of Taq polymerase. The PCR reaction was carried out as 94°C for 30 sec followed by 25 cycles of 94°C for 30 sec and 68°C for 1 min and a final extension step of 68°C for 1 min. After amplification, the purified products were digested by Hind III and Bam HI (TaKaRa, Dalian, China) and ligated into the pET-30a vector (Novagen, Germany). Finally they were transformed into *E. coli* BL21 (DE3) (Tiangen, Beijing, China) by heat shock. Transformed cells were spreaded on LB-kanamycin plates for screening of mutants showing increased activity. The LB-kanamycin plate was composed of 0.5% yeast extract, 1% peptone, 1% NaCl, 1.8% agar and 100 μgm L^{-1} kanamycin.

Library screening: Single colonies from the mutant library were picked with a sterile toothpick and incubated in separate wells of a 96 deep well flat-bottom block which contained 1 mL LB and 100 μg mL^{-1} kanamycin. After growing at 37°C until OD600 was around 0.5, the cells were induced by adding Isopropyl β-D-1-Thiogalactopyranoside (IPTG) to a final concentration of 1 mmol L^{-1} followed by growth at 37°C for 16 h. The cells were harvested by centrifuging (3,000x g, 4°C) for 10 min and the pellets were resuspended in 0.2 mL ice-cold Phosphate-Buffered Saline (PBS, 137 mmol L^{-1} NaCl, 2.7 mmol L^{-1} KCl, 10 mmol L^{-1} Na_2HPO4, 2 mmol L^{-1} KH_2PO4, pH 7.4). Then, 160 μL cell solution from each well was mixed with 40 μL BugBuster™ reagent (Novagen, Germany) and incubated at room temperature for 30 min followed by centrifugation (3000×g, 4°C) for 10 min, non-viscous supernatant was obtained for enzyme assay. Each cell suspension (50 μL) was transferred to another 96 well plate with each well containing 50 μL 1% (w/v) beechwoodxylan (sigma, X0502) in McIlvaine's buffer (pH 5.0). After 20 min incubation at 50°C, the reaction was stopped by adding 100 μL 3,5-Dinitrosalicylic acid (DNS) into the mixture followed by boiled for 10 min (Miller, 1959). The increase in absorbance at 540 nm was determined using SpectraMax M5 (molecular devices). The mutants with higher activity than parent were sequenced by BGI and the genes of these mutants were served as parents for another round of error-prone PCR.

Expression and purification of Wild Type (WT) and mutant enzymes: A single colony of WT and mutants was grown overnight in LB medium containing kanamycin (100 μg mL^{-1}) at 37°C then diluted by 1:100 in 100 mL fresh LB-kanamycin medium and further incubated at 37°C for scale-up culture. The culture was induced by adding 100 μL IPTG (1 mol L^{-1}) when OD_{600} reached 0.6. After 8-9 h, cells were harvested by centrifugation (12,000×g, 10 min at 4°C) and then the pellets were resuspended in 30 mL ice-cold PBS buffer. After disrupting the cells sonication, the lysates were centrifuged at 12,000×g at 4°C for 10 min and then the recombinant protein in the supernatant was purified by Ni-NTA agarose affinity chromatography. The supernatant was charged with 0.7 mL Ni-NTA agarose (Qiagen, Germany) which bound the 6×His-tagged protein followed by 1 h incubation on ice then poured into the affinity column (Bio-Rad, Shanghai, China). The column was washed twice with 20 mL wash buffer (20 mmol L^{-1} imidazole) and once with 1 mL wash buffer (80 mmol L^{-1} imidazole), finally the protein was eluted 4 times with 1 mL elution buffer (250 mmol L^{-1} imidazole). Each wash fraction and elute was collected for sodium dodecyl sulfate-polyacrylamide gel electrophoresis (SDS-PAGE, Laemmli, 1970) and Western-blot analysis.

Measurement of xylanase activity: The activity of xylanase was determined by DNS Method (Bailey *et al*., 1992). D-xylose was used as the standard. Each cell extract in 96 well plate (50 μL) was mixed with 50 μL 1% (w/v) beechwoodxylan (Sigma, X0502) in McIlvaine's buffer (pH 5.0). After incubation at 50°C for 20 min, 100 μL DNS was added to stop the reaction then the mixture was heated at 100°C for 10 min. Reducing sugars were determined at 540 nm on SpectraMax M5 (Molecular Devices). One Unit (U) of xylanase activity was defined as the amount of the enzyme that produced reducing sugar equivalent to 1 μmol of xylose per minute. Protein concentration was estimated using BCA Protein Assay kit from KeyGEN with BSA as the standard (Bradford, 1976).

pH optimum and stability: The effect of pH on xylanase activity was measured over a range of pH 3.0-10.0 (pH 3.0-8.0, McIlvaine's Buffer System; pH 9.0-10.0, 0.2 mol L^{-1} glycine, 0.2 mol L^{-1} NaOH Buffer System; pH 9.0-10.0, 0.2 mol L^{-1} glycine, 0.2 mol L^{-1} NaOH Buffer System) at 50°C. To determine the pH stability, enzymes were incubated in various pH buffers at 37°C for 30 min and the residual activities were estimated under the optimum condition.

Temperature optimum and thermostability: The optimum temperature was determined at pH 5.0 from 30-80°C. Thermostability experiment was performed by assaying the residual xylanase activity after incubation in McIlvaine's buffer (pH 5.0) at 50, 60, 70 and 80°C for 30 min. The residual xylanase activity was estimated under the optimum condition.

Analysis of kinetic parameters: To determine the kinetic parameters of xylanases, the beechwood xylan was used as substrate of which the concentration varies from 0.4-10 mg mL^{-1} in the optimum pH of xylanases. After incubation at 50°C for 5 min, the product of reducing sugars was measured spectrophotometrically at 540 nm. Then, the kinetic parameters (km and Vmax) were calculated via Lineweaver-Burk plot (Lineweaver and Burk, 1934). These assays were performed in triplicate.

Sequence analysis: DNA sequences of the WT and mutants were translated into their protein complements and aligned to identify the mutations of amino acid residues. Protein sequence alignment was performed with DNAMan5.2.2 (http://www.lynnon.com/) and ClusterW2 (http://www.ebi.ac.uk/Tools/msa/clustalw2/). Active sites of WT and mutants were predicted by Pfam (http://pfam.sanger.ac.uk/search). The physicochemical properties of the proteins were computed using Expasy'sprotparam tool (http://www.expasy.org/tools/protparam.html). The disulfide bonds of proteins were predicted by http://clavius.bc.edu/~clotelab/DiANNA/. The dimensional structure of proteins were predicted by I-TASSER(http://zhanglab.ccmb.med.umich.edu/I-TASSER/) (Zhang, 2008; Roy *et al*., 2010, 2012) and the top-scoring models which means a model with the highest confidence were analyzed by Chimera1.7(http://www.cgl.ucsf.edu/chimera/) (Pettersen *et al*., 2004).

RESULTS

Cloning of *xylanase* gene: The gene *ORF6-UN* encoding a 34 kDa xylanase (HA2) was cloned by PCR. The genome sequence was available by Wang *et al*. (2012a). Pfam alignment showed that ORF6-UN was a *xylanase* gene encoding a glycoside hydrolase family 11 xylanase with 61% similarity to the endo-1, 4-β-xylanase of *Fibrobactersuccino* genes S85 (YP_003250510.1).

Mutagenesis of xylanase: After the first round of random mutagenesis and screening, a mutant library consisting of 1450 clones was screened in 96 well plates and 42 clones displaying enhanced absorbance than the parent (HA2) were picked for scale-up culture. However, all clones except C12 exhibited lower activity than the parent and the gene of *C12* was subjected to a second round of random mutagenesis. In this round, 31 of approximately 2500 clones with higher absorbance than C12 were obtained. After scale-up culture, only three clones were identified with higher activity than both C12 and HA2 and the specific activity of E12 was the highest.

Enzyme production and purification: After purification by Ni-NTA agarose affinity chromatography, a single band around 34 kDa was visualized by SDS-PAGE analysis (Fig. 1a) which corresponded well with the estimated molecular mass for the 233 amino acids (HA2, C12 and E12). This result was confirmed by the Western-blot analysis with Anti-His Tag mouse monoclonal antibody (Fig. 1b).

Xylanase activity and kinetic analysis: The specific activity of HA2, C12 and E12 was 59.31, 69.67 and 118.50 Umg^{-1}, respectively (Table 1). The Mutant C12 showed a 78% decrease in km and a 77% decrease in kcat, resulting in approximately a 1.06-fold increase in (kcat/km). Mutant E12 displayed a 4.02-fold increase in km and 4.64-fold increase in kcat leading to a 15% increase in (kcat/km).

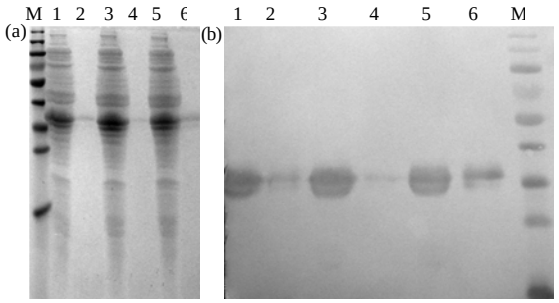

Fig. 1: a) SDS-PAGE and b) Western-blot analysis of HA2, C12 and E12 expressed in *E. coli*; Lane 1, 3 and 5: lysis supernatant from HA2, C12 and E12, respectively; Lane 2, 4 and 6: purified HA2, C12 and E12, respectively; M: standard protein marker from low to up were 17, 26, 34, 43, 55, 72, 95, 130 and 170 kDa

Table 1: Xylanase activity[a] and kinetic constants[b] of HA2, C12 and E12

Xylanases	Specific activity (U mg^{-1})	km (mg mL^{-1})	kcat (1 sec^{-1})	kcat/km (mL/mg/s)
HA2	59.02±1.27	11.22±10.50	42.82±5.10	3.82±0.15
C12	68.03±0.58	2.42±00.14	9.82±0.26	4.06±0.10
E12	120.30±1.19	45.14±13.50	198.75±8.23	4.40±0.09

[a]Xylanase activities were determined at their optimum conditions as described in materials and methods; [b]the concentration of beechwood xylan ranged from 0.4-10 mg mL^{-1}. All these assays were carried out in triplicate

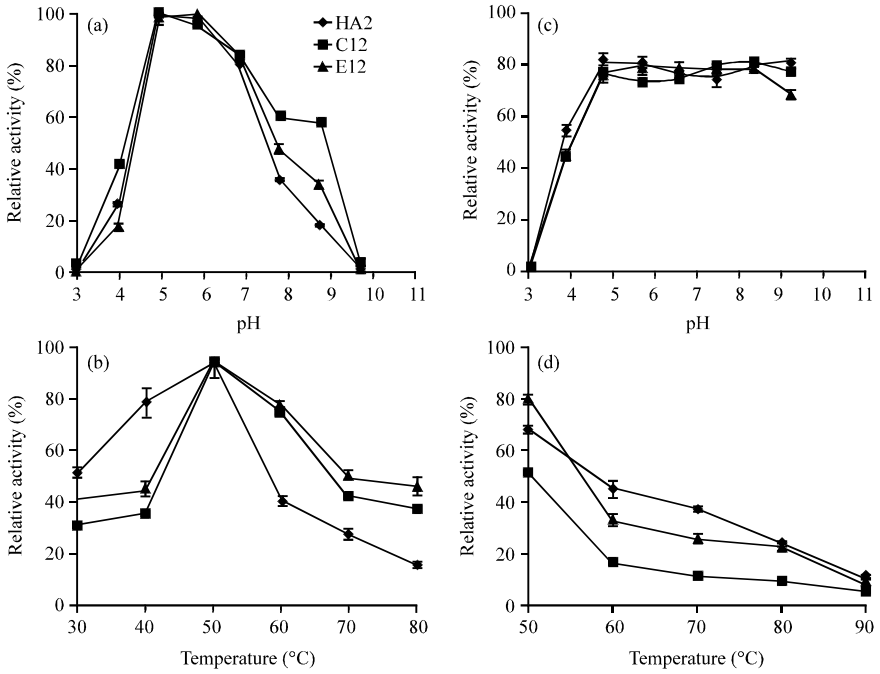

Fig. 2: Characterization of the parent HA2 and mutants C12, E12; a) effect of pHon xylanase activity of HA2, C12, E12; b) effect of temperature on xylanase activity of HA2, C12, E12; c) the pH stability on xylanase activity of HA2, C12, E12; d) thermostability of HA2, C12, E12 at different temperatures. These assays were determined as described in materials and methods using 1% beechwoodxylan as substrate. The highest xylanase activity was taken as 100% in assay of optimum temperature and optimum pH. All the data are given as mean±SE, n = 3

```
C12             DFCQTAAHSGTSRHVTTNTVGSFDNGIGYELWNEGGNGGSATFYDDGSFNCKMTGARDYL 60
E12             DFCQTAAHSGTSRHVTTNTAGSFDNGIGYELWNEGGNGGSATFYDDGSFNCKITGARDYL 60
HA2             DFCQTAAHSGTSRQVTTNTVGSFDNGIGYELWNEGGNGGSATFYDDGSFNCKMTGAKDYL 60
                ************* ***** ******************************** *** ***

C12             CRAGLSFNSDKTHGEIGHMKADFKLVKRNLSGIQYSYIGIYGWTREPLVEWYIVDNTGSD 120
E12             CRAGLSFNSDKTHGEIGHMKADFKLVKRNLSGIQYSYIGIYGWTREPLVEWYIVDNTGSD 120
HA2             CRAGLSFNSDKTHGEIGHMKADFKLVKRNLSGIQYSYIGIYGWTREPLVEWYIVDNTGSD 120
                ************************************************************
                                                                ▲

C12             YMPGDWVAQGNSKKKHGVFKIDGADYTVYEGDRTSYSIDGDGKYFKQYFSVRTSKRDCGT 180
E12             YMPGDWVAQGNSKKKHGVFKIDGADYTVYEGDRTSYSIDGDGKYFKQYFSVRTSKRDCGT 180
HA2             YMPGDWVAQGNSKKKHGVFKIDGADYTVYEGDRTSYSIDGDGKYFKQYFSVRTSKRDCGT 180
                ************************************************************

C12             IDITAHFKKWEELGMKMGKMHEAKILGEAGNSNGAQARGEYDFPYAKVYIEGA 233
E12             IDITAHFKKWEELGMKMGKMHEAKILGEAGNSNGAQARGEYDFPYAKVYIEGA 233
HA2             IDITAHFKKWEELGMKMGKMHEAKILGEAGNSNGAQARGEYDFPYAKVYIEGA 233
                ***********************************************
                           ▲
```

Fig. 3: Alignment of amino acid sequences of HA2 and mutants (C12 and E12); '*' indicates the residues are conserved in the alignment. The two active sites were shown as filled triangle. The alignmentwas done by using ClusterW2 alignment program on the GenomeNet server (http://www.ebi.ac.uk/ Tools/clustalw2/)

Effects of temperature and pH on enzyme activity: The optimum temperature for WT and two mutants were all 50°C (Fig. 2a) although, C12 and E12 displayed lower thermostability than HA2 (Fig. 2d). The E12 was able to retain 80% xylanase activity after exposed to 50°C for 30 min but showed a sharp decrease to 37% in its activity at 60°C. The WT retained only 66% of its original activity at 50°C but its activity reduced >50% when exposed at 60°C for 30 min. The C12 retained only 50% activity at 50°C and 20% at 60°C.

The optimum pH for WT, mutant C12 and mutant E12 was 5.0, 5.0 and 6.0, respectively (Fig. 2b). In the pH stability study, both of WT and mutants retained about 85% of activity arrange from pH 5.0-9.0 (Fig. 2c).

Sequence analysis: Amino acid alignment revealed that C12 was mutated at two positions (Q14H, K57R) and E12 was mutated at four substitutions (Q14H, V20A, M53I and K57R) while these mutations were far from the active sites, E110 and E208 (Fig. 3). The three dimensional structures

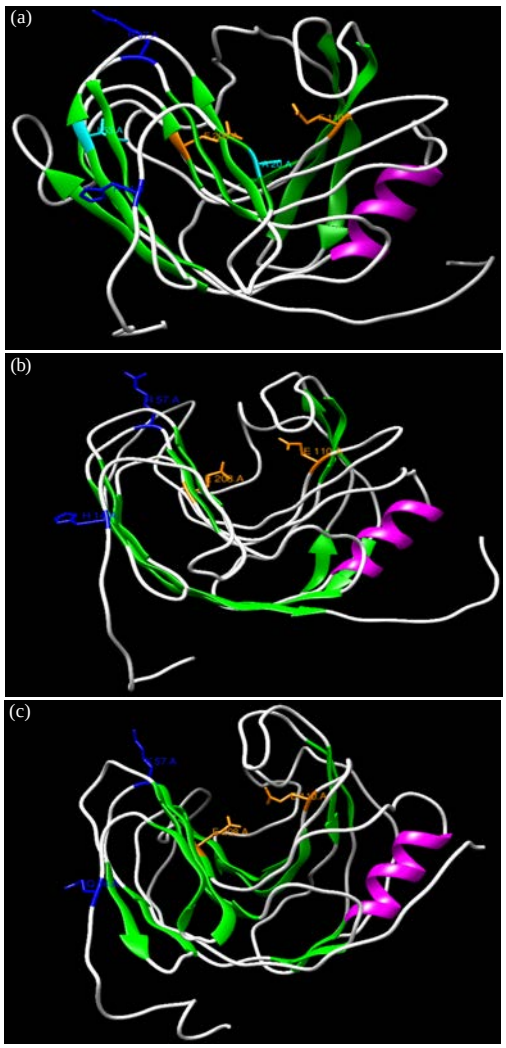

Fig. 4: a) Structure comparison of HA2; b) C12 and c) E12. The catalytic residues (E110 and E208) were in orange, position 14 and 57 were in deep blue, position 20 and 53 were in light blue. The figure was generated by using Chimera 1.7 (http://www.cgl.ucsf.edu/chimera/)

of WT and mutants showed that the two catalytic residues (E110 and E208) were pocketed in the cavity of protein, Q14H, K57R and V20A were substituted within the random coil far from the catalytic residues only M53I substitution was observed within the sheet near the catalytic residues (Fig. 4).

The pI values of the WT and two mutants were in the range of 6.09-6.18. The instability indexes were from 14.25-15.53. Aliphatic index ranged from 52.36-53.22. The GRAVY values were ranging from −0.664 to −0.663 (Table 2).

Table 2: The physicochemical parameters of HA2, C12 and E12 computed using Expasy's Protparam tool

Xylanases	Theoretical pI	Instability index	Aliphatic index	GRAVY
HA2	6.09	15.21	52.36	-0.663
C12	6.18	15.53	52.36	-0.664
E12	6.18	14.25	53.22	-0.663

DISCUSSION

Directed evolution mimics the Darwinian evolution process in the test tube (Cobb *et al*., 2013) which has been widely used to improve or modify the activity and stability of proteins (Brakmann, 2001). In this study, the positive mutation efficiency was quite low, only one in 1450 clones in the first round of random mutagenesis and three in 2500 clones in the second round. The unstable expression in tube might be attributed to distant cell concentration and inadequate shaking (Wang *et al*., 2012a). Compared to WT, mutations of Q14H and K57R increased the affinity of xylanase to substrate (km was reduced by 78%) but decreased catalytic efficiency (kcat was reduced by 79%).

However, further mutation of V20A and M53I reversed the km to 45.14 mg mL^{-1} and kcat to 198.75 sec^{-1} indicating that V20A and M53I might be the key positions for the xylanase activity. A closer view of mutation sites suggested that M53I located near E208 (one of the catalytic residues). After amino acid substitution, isoleucine increased hydrophobic of the enzyme which was supposed to protect activity center from water, beneficial to the acid catalyst to protonate the substrate (Kim *et al*., 2008; Wang *et al*., 2012a).

The disulfide bonds were not changed with the four substitution although, the force of hydrogen bond was weakened by M53I (Fig. 5e and f) it was intensified with the mutations of Q14H (Fig. 5a and b) and K57R (Fig. 5c and d), respectively. Furthermore, the molecular weights of histidine and arginine were larger than those of glutamine and lysine, alanine and isoleucine was smaller than that of V and M which could generate more van der waals force between His14, Arg57 and those residues nearby.

These changes of hydrogen bonds increased the thermostability of C12 and decreased that of E12 which was inconsistent to the decreased thermostability of C12. Therefore, further studies based on site-directed mutagenesis and three-dimensional structure needto be carried out to elucidate the role of each mutation in the enhanced stability and deduced thermostability.

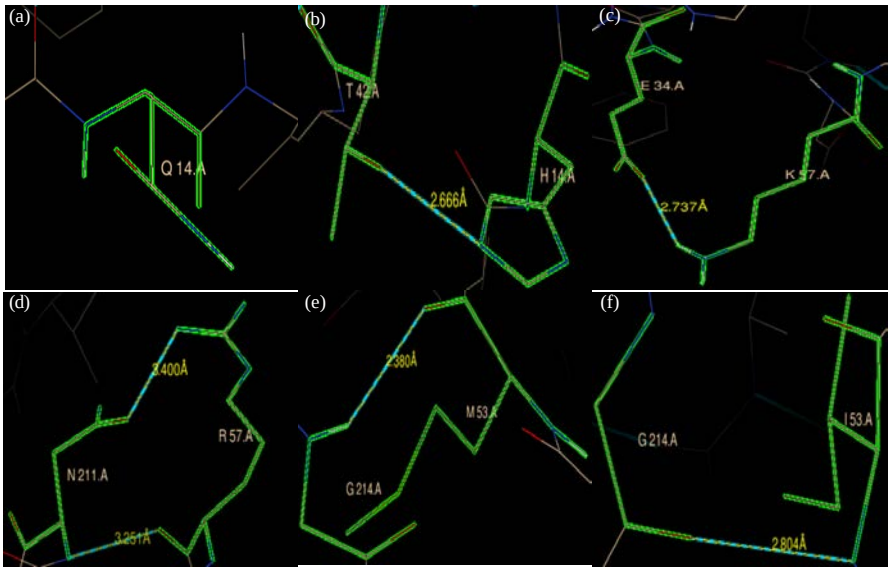

Fig. 5: The change of hydrogen bonds after mutagenesis. All amino acid residues showed above were highlighted and the hydrogen bonds were displayed as blue dashed lines; (a, c, e) were amino acid residues in parental xylanase and (b, d, f) were amino acid residues in mutant xylanases. There was no hydrogen bond in Q14: a) after mutagenesis, one hydrogen bond (with distance of 2.666 Å) was observed between H14 and T42; b) K57 shared one hydrogen bond (with distance of 2.737 Å) with E34; c) whereas two hydrogen bonds (with distance of 3.400 and 3.251 Å) were observed between R57 and N211; d) M53 shared one hydrogen bond (with distance of 2.380 Å) with G214; e) whereas one hydrogen bond (with distance of 2.804 Å) was observed between I53 and G214 and f) the figure was generated by using Chimera 1.7 (http://www.cgl.ucsf.edu/chimera/)

CONCLUSION

The rumen of ruminants is an excellent resource for glycoside hydrolytic enzymes. Error-prone PCR is an effective approach to modify of xylanases without structure informations. After two rounds of error-prone PCR, E12 with the highest catalytic activity of 118.50 U mg^{-1} (about two-fold to its parent) was obtained. Two amino acid substitutions V20A and M53I might be the reason for the enhancement of activity.

ACKNOWLEDGEMENT

This research was supported by grants from the project of International Atomic Energy Agency (IAEA) (RC-16327-R0).

REFERENCES

Bailey, M.J., P. Biely and K. Poutanen, 1992. Interlaboratory testing of methods for assay of xylanase activity. J. Biotechnol., 23: 257-270.

Beg, Q.K., M. Kapoor, L. Mahajan and G.S. Hoondal, 2001. Microbial xylanases and their industrial applications: A review. Applied Microbiol. Biotechnol., 56: 326-338.

Bradford, M.M., 1976. A rapid and sensitive method for the quantitation of microgram quantities of protein utilizing the principle of protein-dye binding. Anal. Biochem., 72: 248-254.

Brakmann, S., 2001. Discovery of superior enzymes by directed molecular evolution. Chembiochem, 2: 865-871.

Cobb, R.E., N. Sun and H. Zhao, 2013. Directed evolution as a powerful synthetic biology tool. Methods, 60: 81-90.

Kim, S.H., S. Pokhrel and Y.J. Yoo, 2008. Mutation of non-conserved amino acids surrounding catalytic site to shift pH optimum of *Bacillus circulans* xylanase. J. Mol. Catal. B, 55: 130-136.

Laemmli, U.K., 1970. Cleavage of structural proteins during the assembly of the head of bacteriophage T4. Nature, 227: 680-685.

Lineweaver, H. and D. Burk, 1934. The determination of enzyme dissociation constants. J. Am. Chem. Soc., 56: 658-666.

Miller, G.L., 1959. Use of dinitrosalicylic acid reagent for determination of reducing sugar. Anal. Chem., 31: 426-428.

Miyazaki, K., M. Takenouchi, H. Kondo, N. Noro, M. Suzuki and S. Tsuda, 2006. Thermal stabilization of *Bacillus subtilis* family-11 xylanase by directed evolution. J. Biol. Chem., 281: 10236-10242.

Pettersen, E.F., T.D. Goddard, C.C. Huang, G.S. Couch, D.M. Greenblatt, E.C. Meng and T.E. Ferrin, 2004. UCSF chimera-a visualization system for exploratory research and analysis. J. Comput. Chem., 25: 1605-1612.

Roy, A., A. Kucukural and Y. Zhang, 2010. I-TASSER: A unified platform for automated protein structure and function prediction. Nat. Protoc., 5: 725-738.

Roy, A., J. Yang and Y. Zhang, 2012. COFACTOR: An accurate comparative algorithm for structure-based protein function annotation. Nucleic Acids Res., 40: W471-W477.

Stephens, D.E., K. Rumbold, K. Permaul, K. Permaul, B.A. Prior and S. Singh, 2007. Directed evolution of the thermostable xylanase from *Thermomyces lanuginosus*. J. Biotechnol., 127: 348-354.

Wang, J., Z. Sun, Y. Zhou, Q. Wang, J.A. Ye, Z. Chen and J. Liu, 2012a. Screening of a Xylanase clone from a fosmid library of rumen microbiota in Hu sheep. Anim. Biotechnol., 23: 156-173.

Wang, Q., L.L. Zhao, J.Y. Sun, J.X. Liu and X.Y. Weng, 2012b. Enhancing catalytic activity of a hybrid xylanase through single substitution of Leu to Pro near the active site. World J. Microbiol. Biotechnol., 28: 929-935.

Zhang, Y., 2008. I-TASSER server for protein 3D structure prediction. BMC Bioinformat., Vol. 9. 10.1186/1471-2105-9-40.